NASA Technical Memorandum 103702
AIAA-91-0253

Turbulent Boundary Layer Separation Over a Rearward Facing Ramp and Its Control Through Mechanical Excitation

Daniel J. McKinzie, Jr.
Lewis Research Center
Cleveland, Ohio

NASA
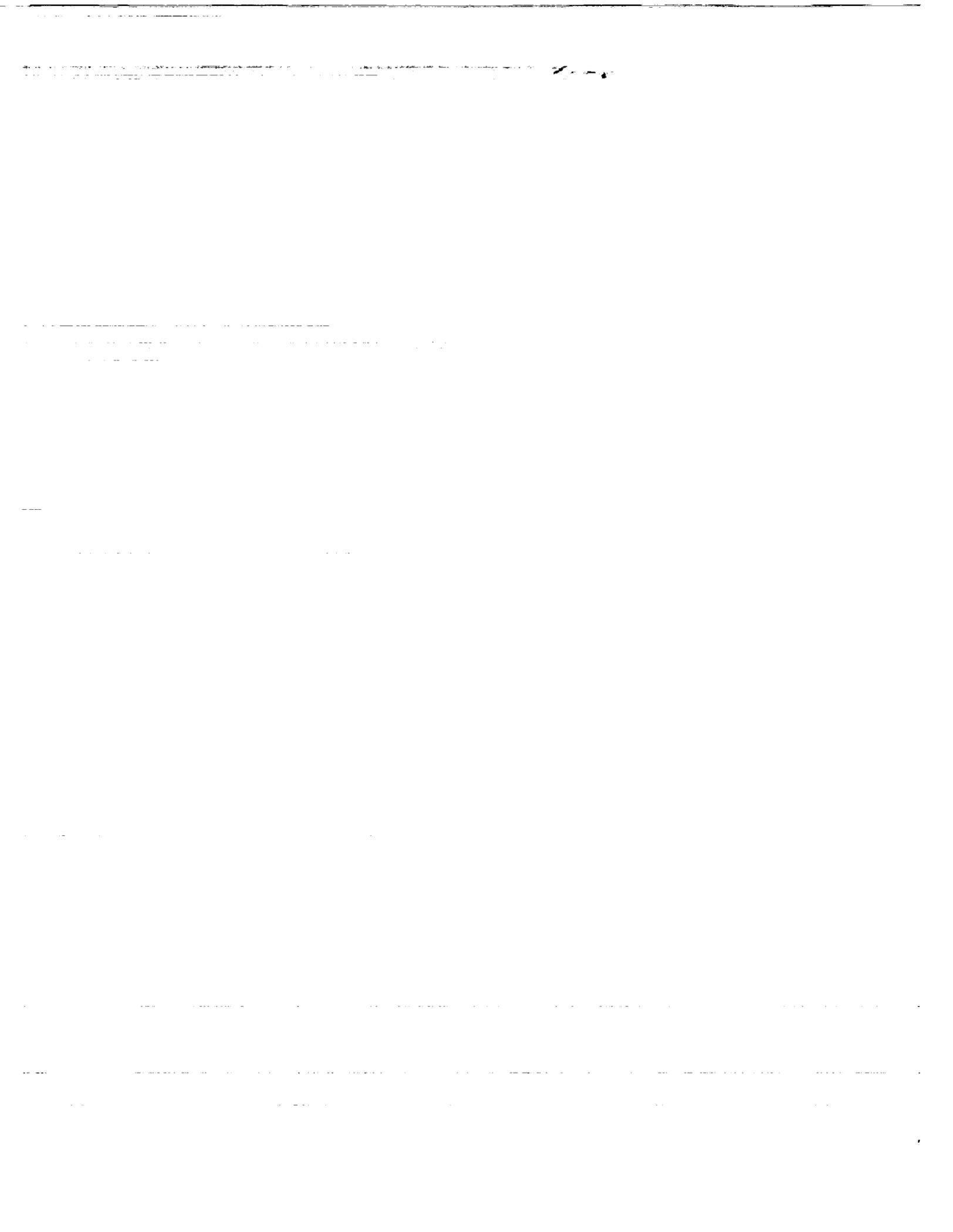
TURBULENT BOUNDARY LAYER SEPARATION OVER A REARWARD FACING RAMP AND ITS CONTROL THROUGH MECHANICAL EXCITATION

Daniel J. McKinzie, Jr.
National Aeronautics and Space Administration
Lewis Research Center
Cleveland, Ohio 44135

SUMMARY

A vane oscillating about a fixed point at the inlet to a two-dimensional 20° rearward facing ramp has proven effective in delaying the separation of a turbulent boundary layer.

Measurements of the ramp surface static pressure coefficient obtained under the condition of vane oscillation and constant inlet velocity revealed that two different effects occurred with surface distance along the ramp. In the vicinity of the oscillating vane the pressure coefficient varied as a negative function of the vane's trailing edge rms velocity; the independent variables on which the rms velocity depends are the vane's oscillation frequency and its displacement amplitude. From a point downstream of the vane to the exit of the ramp, however, the pressure coefficient varied as a more complex function of the two independent variables. That is, it was found to vary as a function of the vane's oscillation frequency throughout the entire range of frequencies covered during the test, but over only a limited range of the trailing edge displacement amplitudes covered. More specifically, the value of the pressure coefficient was independent of increases in the vane's displacement amplitude above approximately 35 inner wall units of the boundary layer. Below this specific amplitude it varied as a function of the vane's trailing edge rms velocity. This height is close to the upper limit of the buffer layer, indicating that the action of the vane is primarily affecting the buffer and viscous sublayers of the boundary layer.

A parametric study was made to determine the variation of the maximum static pressure recovery as a function of the vane's oscillation frequency, for several ramp inlet velocities and a constant displacement amplitude of the vane's trailing edge. The results indicate that the phenomenon producing the optimum delay of separation may be Strouhal number dependent.

Corona anemometer measurements obtained in the inner wall regions of the boundary layer for the excited case reveal a large range of unsteadiness in the local velocities. These measurements imply the existence of inflections in the profiles, which provide a mechanism for resulting inviscid flow instabilities to produce turbulence in the near wall region, thereby delaying separation of the boundary layer.

1. INTRODUCTION

A rearward facing ramp, like a rearward facing step, is a common geometric element used in many flow devices. The rearward facing ramp is particularly important, because it is the fundamental element of diffuser designs. Diffusers, in turn, are components of turbopropulsion systems, wind tunnels, test facilities, etc. In these devices they frequently operate to provide maximum pressure recovery, which has been shown experimentally to occur at conditions approaching transitory detachment. This flow condition becomes particularly critical to off-design or unsteady inlet flow conditions that may produce complete or partial separation. Therefore, in

order to identify favorable as well as adverse flow phenomena that affect separation it is important to experimentally investigate phenomena that control separation. In addition, an understanding of these phenomena could eventually provide design criteria leading to development of a shorter diffuser, and also improved jet engine inlet designs.

1.1 Unsteady Diffuser Flow Studies

Artificially induced large scale flow structures have been employed successfully in the past to improve flow attachment over surfaces.[1] Two examples involve the use of common streamwise vortex generators to control flow over an aircraft wing and to maintain attached flow in large angle diffusers. In each case the mechanism has been hypothesized to involve the creation of streamwise vortices that cause a transfer of energy from the outer flow to the boundary layer. Transverse flow disturbance structures have also been examined as a method to control boundary layer separation. Devices have included: transverse cavities to generate disturbances that delay flow separation over an airfoil to higher angles of attack, spacers to build transverse cavities on diffuser walls, and a transverse standing vortex, driven by a control jet at a fixed position in a diffuser. More recently, spiral shaped rotors mounted in the wall on each side of the channel just upstream of the inlet to a two-dimensional diffuser were used in three test cases in which the half angle of the walls was set at 8°, 12°, and 15°.[1] Each rotor produced a vortex structure that was convected through the diffuser, resulting in an unsteady flow. In addition, the phase angle between the rotors could be controlled. Surface pressures and smoke visualization were the principal measurements made in this study in addition to several vertical mean velocity profiles. The operating mechanism hypothesized by Viets, et al.[1] suggests that the rotors allow flow to turn through the large expansion angle at the inlet to the diffuser, and the vortex structures generated energized the boundary layer allowing it to overcome the larger pressure gradient of the diffuser. Although the pressure recovery improvement was small the study concludes that time dependent flows appear to have potential to improve the performance of the diffusers.

Chen and Shiying, 1989[2] presented experimental measurements for an asymmetric two-dimensional 15° diffuser operated at inlet velocities of 15, 30, and 45 m/sec. The purpose of the investigation was to examine that inherent unsteady wall to wall "flipping" phenomenon of the diffuser separated flow, discussed by Viets, et al.,[1] with the intent of learning how to control it and thus improve diffuser pressure recovery. It was found that a spoiler like flap mounted on the nondivergent wall caused the separation to flip from one wall to the opposite wall, and when coupled with an active control technique (oscillation of the flap) reduced the size of the separation zone and improved the diffuser's performance. Measured data are presented in the form of rms velocity, kinetic energy contours, and a backflow parameter as a function of flap location, displacement amplitude, and frequency of oscillation. The optimum axial mounting location for the flap on the nondivergent wall was found to be opposite the divergent wall where the flow begins to separate. The "flipping" phenomenon was optimized as a function of the flap starting angle, displacement amplitude, and frequency of oscillation. The best control was found when both wall boundary layers separated simultaneously (in phase) which resulted in no mixing of the two wall shear layers at the outlet from the diffuser. Finally by increasing the frequency of excitation above a Strouhal number, S_t, of 0.03 (based on the throat height, t) separation regions were prevented from establishing, thus improving performance.

1.2 Airfoil and Divergent Plate Studies

Two additional experimental studies by Neuburger, et al.[3] and Katz, et al.[4] are of particular interest. Neither one is specifically a study of a rearward facing ramp or diffuser flow. They are however, studies of the delay of separation produced by the introduction of periodic, two-dimensional perturbations into a boundary layer upstream of separation. Neuburger, et al.[3] considered flow passing over an airfoil at large angle of attack,

and Katz, et al.[4] studied turbulent flow passing over a divergent plate connected to an axially oriented splitter plate located in a mixing layer facility. The delay of separation was brought about by a small ribbon or flap positioned upstream of the point of separation, fastened to the surface along its upstream edge and oscillated over a specified frequency range. The purpose of the airfoil study[3] was to prove the hypothesis that the detachment of the shear layer may be delayed to a higher angle of attack by increasing the characteristic width or scale of the eddies generated by the Kelvin Helmholtz instability of a free separated shear layer. This change in the scale of the eddies then is the mechanism by which a change in the rate of entrainment into the separated shear layer occurs, thus delaying separation. More specifically, when the entrained fluid comes from the limited reservoir bounded by the separated shear layer and the solid surface of the airfoil, the pressure is reduced, causing the separated shear layer to bend toward the surface in order to provide the required balance between the curvature of the flow and the pressure gradient in the direction perpendicular to the streamlines. A similar explanation was also provided by E.J. Rice in a private communication in March, 1988 and expanded upon in Rice and Abbott.[5] Flow visualization, surface pressure measurements, and wake surveys to determine the drag coefficients were made for two airfoils in this investigation. The study showed that delay of stall and enhancement of $(Cl)_{max}$ for both airfoils was achieved depending on the geometry of the airfoil, the Reynolds number, location of the vibrating ribbon, and the frequency and amplitude of the imposed oscillation. Proof of the hypothesis was inferred by the pressure coefficient and flow visualization data presented.

Katz, et al.[4] proposes the same mechanism as Neuburger, et al.[3] The study was undertaken to test the concept of this mechanism and its feasibility. A flat plate was hinged at a divergent angle of 18° to a splitter plate oriented axially in a mixing layer facility. The arrangement provided a discontinuity in the pressure gradient which could not be negotiated by the upstream boundary layer, thus the flow separated near this location. A small flap was positioned at the hinge location in such a manner that it could be oscillated. The displacement amplitude of the flap was small and on the order of ±1 mm. Hot wire, local surface pressures, and two point phase locked measurements was made. Katz, et al.[4] present measurements of the variation of the momentum thickness, θ, the shape factor, H, and the skin friction coefficient, C_f, with surface distance as a function of the flap oscillation frequency and displacement amplitude. In addition, a mean velocity profile measured approximately half way along the surface of the divergent flat plate was presented in wall coordinates with the laws of the wall and wake fitted to the data. The separated, unexcited shear layer flow was shown to be the same as that of a classical mixing layer; as such, it could be excited as are mixing layers. The flap was operated at frequencies corresponding to Strouhal numbers based on momentum thickness that were less than 0.01 and flap displacement amplitudes that produced local turbulence intensities of 0.25 percent. These conditions resulted in delay of separation and increases in values of the maximum pressure coefficient approaching 100 percent of the unexcited case. The study concluded that the introduction of harmonic, two-dimensional oscillations results in the delay of separation of the flow and changes the proportions between the "wake" and "wall" functions; it does not, however, alter their universal forms.

In summary, it may be observed that the latter two studies[3,4] demonstrate that a delay of boundary layer separation may be produced by the introduction of lateral two-dimensional forced sinusoidal oscillations into the near wall region at a location very close to the point of the nonforced boundary layer separation. The question might be asked, is there any particular significance in the fact that the forced disturbance signals were introduced into the boundary layer at a location just upstream of, or very close to, the origin of separation of the nonforced boundary layer? The studies reported [1-4] do not provide specific answers to this question, but they do imply that the neighborhood of the boundary layer separation may be the optimum location at which to introduce the forcing disturbance that in turn produces significant effects on the separated shear layer resulting in a delay of separation. It is proposed here that not only is this specific region of the flow field possibly the optimum location to inject the disturbance signal, but in addition, the interaction of the extended downstream boundary layer with the disturbance signals may be of equal importance. Several aspects of these turbulent boundary layer phenomena are discussed below.

1.3 Periodic Flow in Pipes and Channels—Boundary Layer "Bursting" Phenomenon

Kline, et al.[6] and others[7-17] in their studies of the structure of turbulent boundary layer have presented extensive visual and quantitative data for flows experiencing zero, negative, and positive pressure gradients. These studies have revealed the presence of well-organized spatially and temporally dependent motion within the "laminar sublayer." These motions lead to the formation of low-speed streaks in the region very near the wall, and these streaks interact with the outer portions of the flow resulting in sudden oscillations, bursting, and ejection. These processes are believed to play a dominant role in the production of new turbulence and the transport of turbulence within the boundary layers on smooth walls. These studies indicate that the "bursting" phenomenon culminates in "breakup" at a height above the wall in inner wall coordinates, y^+, of approximately 50. Breakup is defined as an amplifying rapid oscillation or sudden instability.

Ramaprian, et al.[15] discuss the phenomena occurring in periodic turbulent pipe and channel flows. Sinusoidal oscillation at moderate to high frequencies were superimposed on the mean flow; the effects of these oscillations on the time-mean, the ensemble-averaged, and random properties of the flow were measured. Results from this study reveal that imposed periodicity plays a significant role in the "bursting" process if the oscillation frequency is higher than a critical frequency. Ramaprian, et al.[15] present a classification scheme for pipe and channel flow in which five regimes of periodic turbulent shear flow are identified and for which unique physical descriptions are offered.

Blackwelder and Swearingen, 1983[18] proposed a mechanism that they believe results in the series of events, which collectively is referred to as the "bursting" phenomenon. They present measured near wall turbulent boundary layer profiles showing points of inflection. The character of the data prompts them to suggest that the spatial inviscid linear stability theory of Michalke[19] may provide a mechanism for explaining the exponential growth rates of disturbances that culminate in the "bursting" phenomenon. They justify this proposal with arguments based on references cited in the literature. One of these arguments concerns the three dimensionality of the near wall region. The use of Michalke's theory is justified in this regard by citing the work of Nishoika, et al.[20] in which the two-dimensional theory is shown to be valid in highly-three dimensional fields. Accordingly a relationship for the frequency of the forced disturbance that will produce the most amplified wave number is presented.[18]

1.4 Present Experiment

In each of the four studies,[1-4] briefly reviewed above, the qualitative description by which the active mechanical methods control the delay of boundary layer separation appear to be similar. The description, however, considers only the action of large scale disturbance structures in the outer region of the boundary layer. It does not explain how the remainder of the boundary layer and, in particular, the inner wall region small scales react/interact with the large scale structures bringing about attached flow resulting in the delay of separation. Therefore, the present experimental program was initiated to study the effect of an oscillating vane on the delay of separation of the boundary layer produced by a 20° rearward facing ramp with the purpose of learning more about the delay of separation mechanism. The program is part of an overall effort at the NASA Lewis Research Center[21,22] to study the effect of controlled disturbances on the natural flow instabilities of several types of turbulent shear layers, with the objective of controlling them. This paper has the following two objectives: first, to present experimental measurements in a study that identified an oscillating vane located on the surface of a rearward facing ramp as an effective active excitation device for the open loop control of turbulent boundary layer separation, and second, to explain qualitatively the phenomena effecting the delay of separation.

2. EXPERIMENTAL FACILITY

2.1 Model and Test Facility

Figure 1 presents a schematic diagram of the ramp attached to an upstream flat plate, positioned within the NASA Lewis 20- by 30-in. Low Speed Wind Tunnel.[23] The flat plate was fabricated from hard wood, using a lamination technique; its surface was smooth and nonlacquered. It was designed to compensate for boundary layer growth resulting in a zero axial pressure gradient at the inlet to the ramp. A cylindrical transition section having a 3.8 cm radius of curvature joins the flat plate to the 20° rearward facing ramp. The surface of the cylindrical transition section was designed to match the radius of curvature of a vane having a 2.54 cm chord and thickness of 0.025 cm. The vane was positioned at the crest of the ramp, attached to the surface along its upstream edge, and was sinusoidally oscillated over a frequency range and peak to peak displacement height, h, of 15 to 33 Hz and from 0.089 to 0.533 cm, respectively. The surface location, at which the vane was located, was arrived at in a series of tests that qualified the vane as an effective separation control device in the present study. The vane actuator mechanism, located within a hollowed out portion of the model, was driven by a precision vibrator located beneath the tunnel. A miniature accelerometer, positioned on the driver push rod mechanism, was used to monitor the frequency and displacement of the vane, thus insuring a smooth sinusoidal wave form. The inphase operation of the vane, its oscillation frequency, and displacement were cross checked optically using strobe equipment. In order to insure a turbulent boundary layer at the inlet to the rearward facing ramp for all test cases presented herein, a 23 cm wide by 76 cm long strip of number 40 sandpaper was positioned well upstream near the crest of the acel/decel ramp-up inlet, as schematically shown in figure 1. The Reynolds number based on momentum thickness was 1200 for a typical case where the inlet velocity to the ramp was 6.6 m/sec.

2.2 Instrumentation

The ramp/flat-plate model was instrumented with 38 axial static pressure taps and 3 spanwise rows of 5 static pressure taps. Flow field and turbulent boundary layer measurements were made using single and cross wire anemometry in addition to a recently developed version of a high voltage corona anemometer.[24,25] A corona anemometer is a device that can measure the speed and direction of a gas by the displacement of an ion beam produced by a corona discharge. It is bidirectional and responds dynamically, therefore, it is especially suited to measure unsteady reversing flow. Data from this probe are presented as contours of averaged flow reversal per unit time that can be used to identify the several stages of unsteady separation discussed by Simpson, et al.[26] The working head of this instrument is shown schematically in figure 2.

3. RESULTS AND DISCUSSION

3.1 Surface Pressure

Typical surface pressure coefficient data, referenced to the upstream inlet conditions to the ramp, are presented in figures 3 and 4 as a function of surface distance, S. The data were obtained for inlet velocities, $\overline{U}_1$, in the range from 2.6 to 10.5 m/sec (Reynolds number per meter from nominally 1.3×10^5 to 6.5×10^5). For the $\overline{U}_1$ of 2.6 m/sec nonexcited case (vane removed, fig. 3) separation occurred at the inlet to the ramp. Oscillating the vane at 23.5 Hz and a peak to peak displacement amplitude, h, of 0.48 cm produced a large reduction of the pressure coefficient at the location of the vane. This was followed abruptly by an equally large increase resulting ultimately in almost 100 percent recovery of the static pressure (ideal pressure recovery, $(P_L - P_1)/q_1 = 0.278$) at the ramp's exit. The 6.6 m/sec inlet velocity case is presented in figure 4. Note that for the nonexcited condition (vane removed) separation did not occur over the entire ramp. This lack of complete

separation agrees, however, with experimental criteria discussed by Chen, et al.[27] Exciting the flow at 29 Hz and an h of 0.533 cm produced a recovery of 88 percent of ideal.

The data presented in figure 5(a) represent a parametric study of the maximum values of the static pressure recovery as a function on excitation frequency, f, for several inlet velocities, $\overline{U}_1$, of 2.6, 4.6, 6.6, and 10.5 m/sec and a constant h of 0.318 cm. For the 2.6 m/sec case the peak recovery occurred at 24 Hz; note the roll-off from the peak at the larger oscillation frequency. At 4.6, 6.6 and 10.5 m/sec a peak did not occur since the oscillator used in the experiment was too weak to maintain the displacement amplitude at higher frequencies. These results show, however, that the optimum excitation frequency increases in some proportional relationship with $\overline{U}_1$. The optimum frequency for the 6.6 m/sec case is approximately 33 Hz, which is based on the observation that the data are approaching the ideal recovery limit. This is close to the so-called most-probable frequency of 30 Hz, which was measured for the same inlet velocity, but nonexcited condition. The most-probable frequency is that frequency that corresponds to the peak in the spectrum of streamwise velocity fluctuations of an unforced mixing layer.

The data presented in figure 5(b) represent a parametric study of the maximum values of the static pressure recovery as a function of h for several inlet velocities, $\overline{U}_1$, of 2.6, 6.6, and 10.5 m/sec and a constant oscillation frequency of 24 Hz. Note that the maximum pressure recovery for all three cases increases with increasing h reaching maxima in the range of h between nominally 0.356 and 0.4 cm. Note also that if the 2.6 m/sec case is excluded, an h of 0.356 cm may well represent the displacement amplitude at which the maxima for the 6.6 and 10.5 m/sec cases occur.

Figure 6 presents a parametric study for the $\overline{U}_1$ case of 6.6 m/sec. Measurements of the pressure coefficient are presented as a function of surface distance, S, for six values of h at constant f (fig. 6(a)), and for six values of f at constant h (fig. 6(b)). Note that the magnitudes of the pressure coefficients at the surface location, S, of 15 cm progressively decrease, first, with increases in h at constant frequency (fig. 6(a)), and second, with increasing oscillation frequency, f, at constant h (fig. 6(b)). Thus the pressure coefficient at this location is clearly dependent on the motion of the vane's trailing edge. Since the vane oscillates in harmonic motion according to the following relationship

$$y_r = \frac{h}{2} \sin(2\pi hT),$$

where T represents time. The fluctuating velocity of the vane's trailing edge may be expressed as

$$v = \frac{\partial y_r}{\partial T} = \pi fh \cos(2\pi fT).$$

And its rms velocity is given by

$$v_{rms} = \frac{\pi fh}{\sqrt{2}}$$

Therefore the vane's trailing edge rms velocity is a direct function of the product of the vane's oscillation frequency and its peak to peak displacement amplitude. Thus the pressure coefficient in the vicinity of the vane's trailing edge appears to vary as a negative function of the vane's trailing edge rms velocity, v_{rms}. At the location of maximum recovery, S of 34 cm, the static pressure recovery varies as a more complex positive function of the two independent variables, f and h. That is, it varies as a positive function of the vane's oscillation frequency, f, throughout the entire range of frequencies tested, but over only a limited range of the trailing edge displacement amplitudes, h, covered. More specifically, from a point near the downstream edge of the vane to

6

the exit of the ramp, the value of the pressure coefficient is independent of increases in the vane's displacement amplitude above approximately 0.318 cm. Below this limiting amplitude it varies as a function of the vane's trailing edge rms velocity. This suggests the possibility that two different responses to the operation of the vane are occurring. One in the neighborhood of the vane and another starting downstream from the vane and persisting to the exit from the ramp. This result is interesting in relationship to measured velocity profiles obtained at several locations within 1.27 cm of the trailing edge of the vane. The profiles reveal coincidently that the inertial sublayer (y^+ of 50) begins at a height above the ramp surface of 0.356 cm. This height is considered close to the "limit" height of 0.318 cm referred to above. Thus the near field action of the vane appears to be primarily affecting the buffer and viscous sublayers of the boundary layer. As mentioned above, Kline, et al.[6] and others[7-17] have identified y^+ of 50 as the location where the "bursting" phenomenon culminates in "breakup". Therefore, the observation may be made that the optimum displacement height at which the vane was operated corresponds closely to a nominal location above the surface which includes the laminar sublayer and some portion of the buffer layer. And further, this location appears to correspond to a point in the boundary layer where the "bursting" phenomenon culminates in "breakup."

At this point it must be mentioned that the effective operation of the oscillating vane was found to be strongly dependent on the trailing edge closing completely down on the ramp's surface. For example, operating at the condition, $\overline{U}_1$, of 6.6 m/sec and with a gap height of 0.058 cm, between the ramp's surface and the lower limit of travel of the vane's trailing edge, resulted in a reduction in the maximum static pressure recovery of 23 percent in comparison to the case in which the vane completely closed down on the surface.

While the mechanisms that explain the data presented in figures 5 and 6 are not completely known at this time, the data appear to indicate that the upstream laminar sublayer and buffer layer are regions in the boundary layer that are of primary importance to the phenomena.

It should also be mentioned that most of the data to be discussed from this point on, are for the case where $\overline{U}_1$ is 6.6 m/sec.

3.2 Flow Reversal Contours

A typical example of the corona anemometer unsteady velocity probability density function versus output voltage (velocity histogram) is presented in figure 7. The data were obtained at a location half way down the length of the ramp at a height above the surface of 0.127 cm. This signal, in plus or minus dc volts, represents an averaged measure of the difference in ion current between the two low voltage (target) electrodes of the probe (see fig. 2). The area under the curve can be processed to determine the average flow reversal per unit time, and the four statistical moments (mean value, variance, skewness, and flatness factor). In addition, the intercepts along the abscissa represent a measured range of the unsteady gas velocity. For the nonexcited case, backflow (up the ramp) is occurring nearly 80 percent of the time. In the event that the backflow was occurring 100 percent of the time, the entire curve representing the probability density function would lie in the negative range of the probe's output voltage. Thus, the unsteady component of the output signal, although fluctuating, would always have a negative value. In the excited case, backflow is occurring for about 35 percent of the time. Thus, the data in figure 7 show that the vane has delayed flow separation and improved the degree of flow attachment at the indicated probe location.

Figure 8 presents contours of the averaged flow reversal rate over the ramp for the nonexcited and excited cases. The inner boundary of these measurements was 0.152 cm above the ramp's surface, well within the inner wall region of the boundary layer. Figure 8(a) presents the nonexcited measurements showing that 100 percent reversal was measured at a point nominally 2.2 cm downstream from the ramp's inlet. The 50 percent reversal contour represents a boundary below which the mean flow velocity is considered reversed; note that this contour

7

is located well above most of the ramp's surface. Thus, from a point nominally 2 cm downstream from the inlet to the ramp to it's exit the mean flow may be considered in a separated state. Figure 8(b) presents the excited case showing that in the inner wall region, from a point nominally 0.64 cm downstream from the vane's trailing edge to the ramp's exit, the flow is attached with a maximum reversal rate of 6 percent near it's exit. These data indicate that while the flow within the inner region of the boundary layer has an unsteady component it is not separated from the ramp's surface at any time with regards to the mean component of the velocity, thus separation, if it exists at all, has been delayed to a point downstream from the exit of the ramp. In summary, figure 8(b) clearly shows that separation was delayed, and also the degree and extent of the attachment for the operating conditions shown.

3.3 Effects in the Vicinity of the Vane

The following is a discussion of the interaction between the oscillating vane and the inner region of the boundary layer fluid passing over it. Since a quantitative description of the vane's interaction with this boundary layer is beyond the scope of the present effort, a discussion follows of the phenomena that have been observed in experimental investigations specifically directed to the study of this interaction.

Ramiz and Acharya[28] studied the unsteady separation introduced into a boundary layer by the motion of a spanwise flap in a pitch-up and hold movement. The undisturbed boundary layer thickness at the flap location was of the order of the flap height. Their objective was to spacially track the separation produced by the flap. The study concluded that the strength and "hold" time of the vortex formed and the features of the ensuing separation are strongly dependent on the rise time of the flap. For longer rise times, a longer time is available for vorticity to accumulate at the tip of the flap. However, the separation region behind the flap also has more time to grow, and is large in streamwise extent when the initial vortex is released from the tip of the flap. As a result, a well-defined vortex is not always seen. In contrast, for a shorter rise time, the initial vortex releases from the flap before the separated region has had time to grow. The vortex is well defined and grows as it convects downstream, as the separated region is established following it.

Nelson, et al.[29] investigated the unsteady, separated flow produced behind a flap for both sinusoidal oscillations and pitch-up and hold motions. The undisturbed boundary layer thickness at the flap location was approximately one and a half flap heights. The objective of the study was to obtain detailed velocity measurements in the unsteady and separated flow region behind the flap with special emphasis on the unsteady reversing flow. The sequence of events that the study revealed for an oscillating flap are as follows. As the flap rises from the wall a strong vortex is formed and negative velocities with magnitudes larger than the free stream are observed. The vortex grows until the flap reaches its maximum extension from the wall. When the flap begins to move back towards the wall, the vortex is released and convects downstream. As Ramiz, et al.[28] also noted, Nelson, et al.[29] describe the phenomena as being strongly dependent on the flap rise time. The size of the vortical region formed behind the flap reduces as the oscillating frequency of the flap is increased. Under low frequency conditions the vortex appears to look like a quasi-steady separated region and a large shear layer is formed starting at the trailing edge of the flap. At the higher frequency condition the size of the shear layer decreases and the unsteady vortex becomes coherent. The presence of the strong coherent vortex induces a region of secondary vorticity of opposite sign upstream of itself.

Miau, et al.[30] investigated the flow phenomena downstream of an oscillating flat plate immersed in a turbulent boundary layer. The purpose of the investigation was to learn how to control separated flow using the unsteady flow structures generated by the oscillating plate in order to enhance the momentum exchange between the free stream fluid and the flow near the wall. The undisturbed boundary layer height at the flap location was 4.5 times that of the extended plate. During the experiment the plate was sinusoidally oscillated over a frequency range from 2 to 15 Hz or in terms of the reduced frequency

8

from 0.0018 to 0.013. Where h represents the width of the plate and $\overline{U}_\infty$ is the free steam velocity at the edge of the undisturbed boundary layer. The experimental results identified a critical reduced frequency near 0.009, which distinguishes two types of flow with different characteristics. Under the subcritical condition the flow showed quasi-steady behavior. That is, a well defined vortex was not always seen at the tip of the plate, but rather a large shear layer was formed. This shear layer flapped up and down in response to the oscillating motion of the plate. Under the supercritical condition, the shear layer shed from the tip of the oscillating plate rolled up into a large scale vortex. Below the tip and closer to the floor of the facility a lower speed volume of fluid was formed into a vortical structure. This vortical structure had an opposite rotational direction and did not release downstream until the plate was retracted toward the flow. This effect became stronger as the reduced frequency was increased. An analysis was performed in order to estimate the magnitude of the critical frequency, however, a comparison with experimental measurements showed it to be in error by a factor of 2. Therefore, the value of the critical frequency number appears to be uncertain, although the concept that a critical frequency exists appears to be well based experimentally.

In summary, the three investigations[28-30] have supported each others' findings. They have established that two types of flows with different characteristics can exist for a sinusoidally oscillating flap, and that the existence of these types of flow are frequency dependent. The direct applicability of these results to the present investigation is not certain. While the nominal Reynolds number range and flap oscillation frequencies are similar between the investigations, the flap configurations are not. In each of the investigations[28-30] discussed above, the flap or plate used was a flat plate that was actuated from a position flat against the floor of the test facility to an extended position perpendicular to the floor. In the present investigation the vane was not a flat plate, but had a 3.8 cm radius of curvature and a chord length of 2.54 cm. It was actuated from a position in contact with the curved surface of the ramp model to an angle of nominally 7.2° above the surface. Thus the vane used in the present test was acting more like a wedge having a small wake, while each plate used in the studies[28-30] acted more like a high drag obstacle. This might be expected to effect differences in the rate of vorticity accumulation and its intensity, but otherwise it is believed the two types of disturbance generators would interact similarly with the boundary layer fluid. A consideration of the experimental measurements obtained during the present study follows.

Figures 9 and 10 present single hot wire mean velocity profiles at locations 0.127 cm upstream and 0.572 cm downstream, respectively, of the vane for the nonexcited case (vane down on the surface) and excited case (vane oscillating at 30 Hz and h of 0.318 cm). For the excited case the vane's trailing edge rms fluctuating velocity was calculated to be 3.2 percent of the local free stream velocity. A comparison of the curves in each figure indicates an increase in the mean velocity within the boundary layer has occurred and that an apparent wall jet exists 0.572 cm downstream from the vane as indicated by the abrupt change in the velocity gradient (fig. 10). The velocity profiles presented in figure 10 are of particular interest because, for the nonexcited case they were obtained just upstream of the boundary layer separation. Also their comparison indicates a complex abrupt change in the velocity gradient occurred for the excited case. This change indicates a change in vorticity that suggests the possibility that two two-dimensional counter rotating vortices maybe present near the wall. This particular aspect is believed important to a qualitative explanation of the phenomena of the delay of separation for the rearward facing ramp considered here. It must be remembered that the initial condition of the flow field considered here is one in which the flow is not excited and the boundary layer is separated from the ramp's surface at a point 2.2 cm downstream from the ramp's inlet. It is this condition that the oscillating vane initially affects. That is, the vane is periodically forming a volume of fluid containing accumulated vorticity that may or may not roll-up to form a vortex. In either case the periodically formed volume leaves the vicinity of the vane and is convected downstream. The growth and evolution of this disturbance volume, as it interacts

9

with the stability characteristics of the free shear layer, eventually effects changes in the free shear that cause the location of separation to be delayed to another location downstream.

For the excited case, both single and cross wire measurements of the turbulence intensity at an axial distance downstream from the vane of 0.572 cm were obtained. The peak turbulence intensities had nominal values of 32 percent of the local free stream velocity; in terms of the local axial velocity component, U, this value rises to 69 percent. This level is considered high. It should be kept in mind in the following discussion that for the excited case presented in figures 9 and 10 the vane is oscillated at 30 Hz, which is the most-probable frequency of the nonexcited shear layer, as discussed previously in section 3.1. The significance of a strong disturbance signal at the most-probable frequency of the nonexcited free shear layer is perhaps best explained by reviewing briefly the work of Ho and Huang.[31] They present a study of the evolution of the coherent structures of a forced free two-dimensional mixing layer. The mixing layer was formed by two steams of flow at different velocities mixing downstream of the trailing edge of a splitter plate separating the streams. The disturbance signal was produced by perturbing the flow rates of each stream upstream of the splitter plate's trailing edge. Velocity perturbations were generated only in the streamwise direction. Downstream of the trailing edge, transverse velocity perturbations appeared along with the streamwise velocity perturbations. Ho and Huang[31] explain that this was due to the curvature of the stagnation streamline that varied in time in order to accommodate the condition of continuity of pressure across the mixing layer. Thus when the mixing layer is periodically forced, coherent structures develop periodically owing to the streamwise and transverse velocity perturbations. Therefore, in the study by Ho and Huang[31] the forcing disturbance was not produced by the action of an oscillating plate that introduced vorticity directly into an evolving shear layer downstream of the plate's trailing edge, as was the case in the three oscillating flat plate studies.[28-30] Ho and Huang[31] proceed to show that the stability of the mixing layer flow and the forcing function play important roles in determining the initial formation of vortices and their evolution as they are convected downstream. A relationship between the forcing function and the stability of the mixing layer is expressed as a function of the forcing frequency, the response frequency, and the calculated most amplified frequency. This relationship then provides clues to the understanding of the formation of vortices and the multiple-vortex-merging phenomenon that occurs as the vortices are convected downstream by the fluid. A mode index relationship between the forcing frequency, f_f, and the response frequency, f_r, is given by

$$f_f = \frac{1}{M} f_r,$$

where M represents the Mth subharmonic of the response frequency, and is selected by the mixing layer. This study reveals that if a forcing signal, having the most-probable frequency of the nonexcited mixing layer, is introduced into the mixing layer then the response frequency of the mixing layer will also equal the forcing frequency. This condition is identified by indicating that the shear layer is operating in the M = 1 mode. If the forcing level is high then the mixing layer forms a strong vortex quickly, and, in addition, the processes leading to multiple-vortex-merging are suppressed for a long distance.

Consideration of the results of the three boundary layer flap interaction studies[28-30] and that of Ho and Huang[31] can serve as a basis for providing insight into the interaction between the boundary layer fluid and the oscillating vane used in the present effort. Therefore, the following events would be expected to take place based on these insights. As the curved vane rises from the inlet surface of the 20° ramp and penetrates the boundary layer vorticity is accumulated at its trailing edge. If the critical frequency at which a vortex forms immediately is greater than the 30 Hz oscillation frequency of the vane, for the specific case considered here, it is expected that the flow would show a quasi-steady behavior. That is, a well defined vortex would not necessarily form at the vane's trailing edge, but rather a shear layer would form that flaps up and down in response to the oscillating motion of the vane. Since the 30 Hz forcing frequency is also equal to the most-probable frequency of the nonexcited separated shear layer Ho and Huang[31] indicate that the shear layer would be

expected to function in the M - 1 mode. Thus, the 30 Hz flapping motion of the shear layer formed at the vane's trailing edge would interact strongly with the stability characteristics of the separated shear layer at its most-probable frequency causing coherent structures to develop as this flapping disturbance grows and is convected downstream of the vane. Since, in addition, the forcing level is high strong vortices would be expected to form quickly, and the processes leading to multiple-vortex-merging would be suppressed for a long distance. Alternately, if the vane's 30 Hz frequency of oscillation is above the critical frequency the shear layer shed from the vane's trailing edge would be expected to roll-up into a vortex immediately with the possibility of a secondary vortex of opposite rotation formed below and upstream of it, as described by Miau, et al.[30] The events following this would be expected to be similar to those presented above for the subcritical case. In summary, both of these descriptions suggest that a strong vortex would likely be formed either immediately at the trailing edge of the oscillating vane, as in the supercritical case, or delayed slightly, as in the subcritical case. The measured data presented up to this point has been that obtained in the immediate and near vicinity of the oscillating vane, now consider additional measured data obtained farther downstream of the vane's trailing edge.

Corona anemometry data presented in figure 11(a) of the unsteady velocity obtained at 0.476 cm downstream from the oscillating vane and at a height of 0.152 cm show a distinct wave form. Probability density data presented in figure 12 were measured downstream from the vane's trailing edge at 0.476 and 1.746 cm and a height of 0.152 cm. These data show two distinct peaks indicating a relatively low noise sinusoidal signal is being measured; note the large range in unsteady voltage present. Typical smoke wire visualization data obtained for the 2.6 m/sec case are presented in figure 13(a) and (b). The nonexcited case is presented in figure 13(a), where the wire was located upstream of the inlet to the ramp and the vane was removed from the model. Note the boundary of the separated region over the ramp. The excited case is presented in figure 13(b), where the wire is located at a point nominally 2.5 cm downstream from the vane's trailing edge. These data clearly show that the oscillating vane produces vortices, and that these vortices show rapid growth as they convect down the ramp. Based on this evidence, it appears reasonable to conclude that the velocity profile presented in figure 10 for the excited case includes the effects of the steady passage of vortices.

Cross wire anemometry data presented in figures 14 and 15 at a position 0.572 cm downstream from the vane's trailing edge present dimensionless turbulent kinetic energy and Reynolds shearing stress levels of 10 and 1.8 percent of the mean flow kinetic energy, respectively, that are produced within the lower 10 percent of the boundary layer, in the near wall region. These data indicate that the local boundary layer is indeed attached. The negative Reynolds stresses, $-uv/(U_\infty)^2_L$, presented in figure 15 appear to be caused by the large coherent structures produced by the oscillating vane, which is operating in the M - 1 mode where vortex pairing is suppressed. Oster and Wygnanski[32] indicate that negative Reynolds stresses were produced in a region of a flow field they investigated in which vortex pairing was suppressed, as it is in the present investigation. They also note that negative Reynolds stresses may be associated with the inclination of the large structures.

As noted in section 3.1 the effective operation of the oscillating vane was found to be strongly dependent on the trailing edge closing completely down on the ramp's surface. The reason for this is not completely understood, but it seems reasonable to suggest that it involves the interaction of the flow field in the vicinity of the vane, including its vortical structure, with the surface of the ramp. The data presented in figures 14 and 15 indicate that high levels of turbulent energy are being produced in the near wall region by the action of the vane. This result appears to be explained by the theoretical analyses presented by Chu, et al.[10] and Walker, Doligalski, and Ersoy,[33-35] which are studies of the response of a wall boundary layer to the motion of several different configurations of convected vortices approaching a wall nearby. They consider the resulting flow field induced by the interaction of the vortices with each other and the local fluid as the vortices approach a wall. The configurations include both single and pairs of two-dimensional vortices. Doligalski and Walker[33] consider the response to a single two-dimensional vortex. They indicate that such an interaction produces a secondary vortex in an unsteady separation and subsequent interaction phenomenon; in addition, explosive boundary layer

growth is to be expected near these vortices. They note that their results suggest that the boundary layer will erupt into the inviscid region in a strong viscous-inviscid interaction.

Figures 16 and 17 present velocity profile data downstream from the vane's trailing edge at locations of 0.476 and 1.746 cm, respectively. Included in these figures are corona anemometer point measurements that include a mean value and range of velocities representing the unsteadiness of the local flow. Local unsteady velocities ranging from ±15 to ±37 percent of the local free stream velocity are present. These measurements clearly show that the range of the unsteady velocity is large, implying that inflections in the profiles exist. These data once again confirm that a strong forcing function and the stability reaction of the flow are producing strong mixing phenomena in the near wall region.

3.4 Velocity Profiles - Laws of the Wall and Wake

Figures 18 and 19 present velocity profile data obtained downstream from the trailing edge of the vane at locations of 1.746 cm and 17.1 cm, respectively, in the form of inner wall variables, u^+ and y^+. The velocity profile data are compared to curves representing three different regions of a turbulent boundary layer. The innermost region, the viscous sublayer, is dominated by viscous shear and is self-similar for all turbulent boundary layers. It is described by

$$u^+ = y^+$$

Where u^+ and y^+ are a function of u_*, which is the friction velocity. Outside of the sublayer, but close to the wall the velocity is logarithmic and is described by

$$u^+ = \frac{1}{K}\ln(y^+) + C$$

where K and C are assumed here to equal 0.41 and 5, respectively. Collectively, these equations representing the sublayer and logarithmic layer are called the "law of the wall." Streamwise pressure gradients have only small effects on this region. Outside of the wall region, the streamwise pressure gradients are important and the velocity profile exhibits a wave-like form. In 1956 Coles[36] presented an equation for the wake region called the "law of the wake." His equation included a wave-like function added to the logarithmic equation. This equation is referred to here as the law-of-the-wake and is written as

$$u^+ = \frac{1}{K}\ln(y^+) + C + \frac{\Pi}{K}W\left(\frac{y}{\delta}\right)$$

where $W(y/\delta) = 2\sin^2(\pi y/2\delta)$, and the wake parameter Π brings in the effect of the streamwise pressure gradient.

The analysis of the turbulent boundary layer presented in figures 18 and 19 included a fit of the data to the law-of-the-wake. The procedure used was based on the work of Deutsch and Zierke.[37] A least-squares fit of the data to the law-of-the-wake was chosen with u_* and Π as the variables to be determined. An error analysis was performed resulting in two second order partial differential equations that were solved simultaneously for u_* and Π to give the minimum squared error. The profile of figure 18 is unique, and not predicted by the law-of-the-wake, although the law-of-the-wall still appears to apply. Note that a second region starting at y^+ of nominally 65 is logarithmic. These are joined by a transition region that corresponds, in the dimensioned profile of figure 17, to a linear variation of U with y. The data presented in figure 19 measured near the exit of the ramp show good agreement with the law-of-the-wake.

12

In summary, in figure 18 the lack of agreement between the law-of-the-wake and the measured data is most probably due to two causes. First, the effects produced by the large forcing disturbances introduced into the inner region of the local boundary layer at the location of the oscillating vane, and second, the local adverse pressure gradient experienced by the mean flow as it passed over the ramp. In figure 19, the large effects of the forcing disturbance and the adverse pressure gradient experienced by the mean flow are revealed by the break-away of the law-of-the-wake at small values of y^* from the law-of-the-wall. Finally, it may be observed, as was done by Katz, et al.[4] that for the excited case in which a strong forcing signal was used to control the delay of separation, the law-of-the-wall remains valid along the ramp's surface while the wake component appears to alone show the effect of forcing. It should be pointed out that the disturbance signal used in the test results presented here was approximately three times larger than the largest disturbance signal reportedly used by Katz, et al.[4] When comparing the two results this difference has manifested itself by a reduction in the magnitudes of u^* and y^* at which the wake component has caused the law-of-the-wake to deviate from the law-of-the-wall.

3.5 Phase and Coherence

Figure 20 presents the variation of the phase angle, ϕ, measured at 30 Hz with axial surface distance, L, downstream from the vane's trailing edge. These data were measured for the test case $\overline{U}_l$ of 6.6 m/sec, an oscillating vane disturbance signal, f, of 30 Hz, and h of 0.318 cm. They were obtained from cross spectral measurements at points above the surface corresponding to 40 percent of the local free stream velocity, $(U_\infty)_L$. In addition, a local value of the coherence is presented in brackets adjacent to each data point. Also, estimates of the local dimensionless phase speed, $C_{ph}/(U_\infty)_L$, of the disturbance and wave length, λ, are presented. An apparent discontinuity in the slope of the data is shown at a point 7.5 cm, downstream from the vane's trailing edge; notice the reductions in the magnitude of the coherence at this same location. Following this, a rise occurred in coherence near the ramp's exit.

Figure 21 presents spanwise variations of the phase angle of the 30 Hz disturbance signal at three axial locations from the vane of 0.48, 4.44, and 8.26 cm. They show that the spanwise structure is nominally two-dimensional for about one-half wave length ($\lambda/2 = 5$ cm) of the sinusoidal excitation signal. At the third axial location of 8.26 cm, notice that three-dimensional effects appear to be taking place as evidenced by the large scatter in the data, suggesting that axial structures are present. These data support the smoke wire visualization data presented in figure 13(b) of well defined rapidly growing spanwise vortices in the boundary layer that persisted to a point nominally halfway down the ramp.

3.6 Effect of Strong Periodic Flow

As discussed above, Ramaprian, et al.[15] studied the phenomena occurring in periodic turbulent pipe and channel flow in which sinusoidal oscillations, at moderate to high frequencies, were superimposed on the mean flow. Figure 22, taken from this study,[15] is a presentation of a classification scheme in which five regimes of unsteady turbulent shear flow are identified. These regimes are correlated by the parameter

$$\frac{2\omega\delta}{\overline{u}_*}$$

where ω represents the radial frequency of oscillation, δ represents the local boundary layer thickness, and $\overline{u}_*$ is the mean local friction velocity. The regimes are classified as a function of this parameter versus Reynolds number, which is based on the local boundary layer thickness, δ. Data from the present experimental measurements obtained at $\overline{U}_l$ of 6.6 m/sec, h of 0.318 cm and f of 30 Hz are included in the figure and lie

in regime V. Regime V is described as one in which the interaction between the imposed oscillations and the turbulent structure will be very strong, and one in which the effect of the periodic flow will be confined to a very thin layer near the wall. Power spectral measurements obtained in the near wall region at axial surface locations between the trailing edge of the vane and the ramp's exit are presented in figure 23. These data include for comparison the nonexcited and excited power spectra at a location 0.48 cm from the vane's trailing edge and at a height of 0.152 cm above the surface of the ramp. In addition, excited data are presented that were obtained at 1.9, 9.5, and 17.1 cm from the vane's trailing edge and at a height of 0.152 cm. The data show a dominant narrow band signal at the vane oscillation frequency of 30 Hz, and indicate that this disturbance signal is dominant and persists in the near wall region of the flow field along the entire surface of the ramp. At the location, L, of 0.48 cm note the broad distribution of energy in the subharmonic and harmonic narrow bandwidths; and at larger distances along the ramp, the subharmonic and higher harmonics are suppressed. In summary, the description of regime of the classification scheme[15] appears to agree with the measured data presented in figures 9 to 11, 13 to 16, and figure 23.

3.7 Near Wall Turbulence Production

Blackwelder and Swearingen[18] proposed a mechanism that they believe results in the "bursting" phenomenon, as discussed previously in section 1.3. They present near wall instantaneous turbulent boundary layer profiles showing points of inflection below y^+ of 50 inner wall units. These data prompted them to present arguments that show the spatial inviscid linear stability theory of Michalke[19] may provide a mechanism for explaining the "bursting" phenomenon. If the mechanism proposed by Blackwelder, et al.[18] culminates in the "bursting" phenomenon in the near wall region, where three-dimensionally dominates the nonforced boundary layers considered by them, then the strong two-dimensional driving mechanism characteristic of the oscillating ribbon and flap discussed by Katz, et al.[4] and Neuburger, et al.[3], respectively, and the vane, described herein, might be expected to enhance the two-dimensional spanwise nature of the flow field producing the more idealized conditions that the linear stability theory is based on. This enhanced spanwise flow field would also provide the mechanism by which a sinusoidal signal of sufficient strength and at the proper frequency could excite the near wall region into enhanced turbulence production, which is a by-product of the "bursting" and "breakup" phenomena. Assuming this to be the case then, according to Blackwelder, et al.[18] the frequency of the forced disturbance that will produce the most amplified wave number is given by the relation

$$\alpha_r \Delta = 0.40.$$

where

$$\alpha_r = \frac{2\pi f}{C_{ph}},$$

C_{ph} represents the phase velocity, and 2Δ is the vorticity thickness of the shear layer. The frequency, therefore, is given by

$$f = \frac{0.40 C_{ph}}{2\pi\Delta}.$$

Evaluating the frequency, f, for the axial location 0.476 cm downstream from the vane, and the nonexcited condition $\overline{U}_1 = 6.6$ m/sec, it is found to equal 29 Hz. This frequency is surprisingly close to that corresponding to first, the measured most-probable frequency of the nonexcited flow field (f = 30 Hz) and second, the peak value of the measured pressure recovery data presented in figure 5(a) (f = 33 Hz). If the spatially growing disturbances in the near wall region of the boundary layer (bursting phenomenon) may be explained by

14

Michalke's spatial linear stability theory, as proposed by Blackwelder, et al.,[18] then this may explain the improvement in the maximum static pressure recovery with increased excitation frequency noted in the measured data presented in figure 5(a); and in particular, that measured for the 2.6 m/sec test case where an apparent peaking occurred at 24 Hz followed by a roll-off from this peak at higher forced oscillation frequencies.

3.8 A Qualitative Explanation of the Delay of Separation

In summary, a qualitative explanation of the delay of turbulent boundary layer separation of flow passing over a 20° rearward facing ramp through the mechanism of an oscillating vane is as follows: A strong two-dimensional periodic vortical disturbance is injected directly into the inner wall region upstream of the detachment location of a separating turbulent boundary layer. The disturbance is produced by the periodic sinusoidal oscillation of a spanwise vane located near the crest of the ramp and attached to the surface on its upstream edge. The vane is believed herein to effect two responses in the evolving flow field. The first, in the immediate vicinity of the vane, is to enhance the large scale structures of the outer region of the boundary layer that dominate the flow features there and control the entrainment of fluid from the limited reservoir bounded by the separated shear layer and the solid surface of the ramp. At the same time it increases the production of turbulent kinetic energy in the inner wall region required to overcome the large mean flow strain rates distributed over the curved surface of the ramp inlet, with the immediate result of delaying separation of the boundary layer. The second effect occurs farther downstream along the flat surface of the ramp. There the periodic fluctuating disturbances and secondary disturbances produced by the vane also produce inflections in the inner wall boundary layer velocity profiles. These inflections, as discussed by Blackwelder, et al.,[18] are believed to be the source of inviscid flow instabilities. The resulting actions of the instabilities collectively constitute the "bursting" phenomenon,[18] and the "bursting" phenomenon in total is the source of turbulence production in the inner layer that promotes attachment of fluid as it passes over the flat surface of the ramp, all the while experiencing an adverse pressure gradient. Since the vane's oscillation frequency may be controlled, the sinusoidal periodic disturbance signal may be tuned to produce the most effective disturbance signal in accordance with the Michalke spatial linear stability theory and its Strouhal number dependence. Perhaps this later effect represents a new aspect in the overall phenomena that constitute the delay of separation studied here. If so, it has revealed not only that turbulence production is important in the physics of the phenomena, but there also exists a disturbance signal frequency aspect relating to the response of the inner wall layer inviscid flow instabilities to the amplification rate versus Strouhal number dependence of Michalke's linear theory of stability.

4. CONCLUDING REMARKS

A vane oscillating about a fixed point at the inlet to a two-dimensional 20° rearward facing ramp has proven effective in delaying the separation of a turbulent boundary layer.

Measurements of the ramp surface static pressure coefficient obtained under the condition of excitation and constant inlet velocity revealed two different effects occurred with surface distance along the ramp. In the near vicinity of the oscillating vane the pressure coefficient varied as a negative function of the vane's trailing edge rms velocity; the independent variables on which the rms velocity depends are the vane's oscillation frequency and its displacement amplitude. At the exit of the ramp, however, the pressure coefficient varied as a more complex positive function of the two independent variables. That is, it was found to vary as a positive function of the vane's oscillation frequency throughout the entire range of frequencies covered during the test, but over only a limited range of the trailing edge displacement amplitudes covered. More specifically, from a point nominally 2 cm downstream of the vane's trailing edge to the exit of the ramp, the value of the pressure coefficient was found to be independent of increases in the vane's displacement amplitude above approximately 35 inner wall units of the boundary layer. Below this specific amplitude it varied as a function of the vane's

trailing edge rms velocity. This height is close to the upper limit of the buffer layer, indicating that the action of the vane is primarily affecting the buffer and viscous sublayers of the boundary layer. It was also found essential that the vane close completely down on the ramp's surface for maximum effectiveness, emphasizing once again the importance of the inner wall region of the boundary layer to the mechanism responsible for the phenomenon.

A parametric study was made to determine the variation of the maximum values of the static pressure recovery measured near the exit of the ramp as a function of the vane's oscillation frequency. This study was made for several ramp inlet velocity conditions and a constant oscillating vane displacement amplitude. The resulting curves displayed a peak value in the maximum static pressure recovery as a function of the vane's oscillation frequency. The frequencies corresponding to these maxima were found to vary in some proportional relationship with the inlet velocities to the ramp. This finding indicates that the phenomenon producing the optimum delay of separation may be Strouhal number dependent.

Finally, for the excited cases, corona anemometer measurements in the inner wall regions of the boundary layer along the surface of the ramp reveal a large range of unsteadiness in the local velocities. These measurements imply the existence of inflections in the profiles, which provide a mechanism for resulting inviscid flow instabilities to produce turbulence in the near wall region. It is believed that this mechanism provides a means for selected periodic disturbances, introduced into the inner wall region, to excite specific inviscid flow instabilities that will optimize the production of turbulence and thereby aid in the delay of the boundary layer separation. Perhaps, this effect represents a new aspect in the overall phenomena that constitute the delay of separation.

A qualitative explanation of the phenomena of delay of separation is made and appears to be supported by the surface static pressure and flow field measurements presented here.

REFERENCES

1. Viets, H.; Ball, M.; and Bougine, D.: Performance of Forced Unsteady Diffusers. AIAA Paper 81-0154, Jan. 12-15, 1981.

2. Chen, D.; and Shiying, Z.: Control of Separation in Diffusers Using Forced Unsteadiness. AIAA Paper 89-1015, Mar. 1989.

3. Neuburger, D.; and Wygnanski, I.: The Use of a Vibrating Ribbon To Delay Separation On Two-Dimensional Airfoils: Some Preliminary Observations. Workshop II on Unsteady Separated Flow, FJSRL-TR-88-0004, 1987. (Avail. NTIS, AD-A202021).

4. Katz, Y.; Nishri, B.; and Wygnanski, I.: The Delay of Turbulent Boundary Layer Separation By Oscillatory Active Control. Phys. Fluids A, vol. 1, no. 2, Feb. 1989, pp. 179-181.

5. Rice, E.J.; and Abbott, J.M.: Control of Flow Separation and Mixing by Aerodynamic Excitation. NASA TM-103131, 1990.

6. Kline, S.J., et al.: The Structure of Turbulent Boundary Layers. J. Fluid Mech., vol. 30, pt. 4, Dec. 22, 1967, pp. 741-773.

7. Karlsson, S.F.: An Unsteady Turbulent Boundary Layer. J. Fluid Mech., vol. 5, pt. 4, May 1959, pp. 622-636.

8. Falco, R.E.: Structural Aspects of Turbulence in Boundary Layer Flows. Turbulence in Liquids, G.K. Patterson and J.C. Zakin, eds., Univ. of Missouri, Rolla, MO, 1979, pp. 1-15.

9. Rao, K.N.; Narasimha, R., and Narayanan, M.A. Badri: The Bursting Phenomenon in a Turbulent Boundary Layer. J. Fluid Mech., vol. 48, pt. 2, July 28, 1971, pp. 339-352.

10. Chu, C.C.; and Falco, R.E.: Vortex Ring/Viscous Wall Layer Interaction Model of the Turbulence Production Process Near Walls. Exper. Fluids, vol. 6, no. 5, 1988, pp. 305-315.

11. Blackwelder, R.F.; and Haritonidis, J.H.: Scaling of the Bursting Frequency in Turbulent Boundary Layers. J. Fluid Mech., vol. 132, July 1983, pp. 87-103.

12. Bogard, D.G.; and Tiederman, W.G.: Burst Detection with Single-Point Velocity Measurements. J. Fluid Mech., vol. 162, Jan. 1986, pp. 389-413.

13. Gad-El-Hak, M.; and Hussain, A.K.M. F.: Coherent Structures in a Turbulent Boundary Layer. Part I. Generation of "Artificial" Bursts. Phys. Fluids, vol. 29, no. 7, July 1986, pp. 2124-2139.

14. Tu, S.W.; and Ramaprian, B.R.: Fully Developed Periodic Turbulent-Pipe Flow. Part I. Main Experimental Results and Comparison with Predictions. J. Fluid Mech., vol. 137, Dec. 1983, pp. 31-58.

15. Ramaprian, B.R.; and Tu, S.W.: Fully Developed Periodic Turbulent Pipe Flow. Part 2. The Detailed Structure of the Flow. J. Fluid Mech., vol. 137, Dec. 1983, pp. 59-81.

16. Mao, Z.X.; and Hanratty, T.J.: Studies of the Wall Shear Stress in a Turbulent Pulsating Pipe Flow. J. Fluid Mech., vol. 170, 1986, pp. 545-564.

17. Parikh, P.G.; Reynolds, W.C.; and Jayaraman, R.: Behavior of an Unsteady Turbulent Boundary Layer. AIAA J., vol. 20, no. 6, June 1982, pp. 769-775.

18. Blackwelder, R.F.; and Swearingen, J.D.: The Role of Inflectional Velocity Profiles in Wall Bounded Flows. Near Wall Turbulence. S.J. Kline, and N.J. Afgan, eds., Hemisphere Pub. Corp., 1989, pp. 268-288.

19. Michalke, A.: On Spatially Growing Disturbances in an Inviscid Shear Layer. J. Fluid Mech., vol. 23, pt. 3, Nov. 1965, pp. 521-544.

20. Nishioka, M.; Asai, M.; and Iida, S.: An Experimental Investigation of the Secondary Instability. Laminar-Turbulent Transition. R. Eppler and H. Fasel, eds., Springer Verlag, Berlin, 1980, pp. 37-46.

21. Stone, J.R.; and McKinzie, Jr., D.J.: Acoustic Excitation - A Promising New Means of Controlling Shear Layers. NASA TM-83772, 1984.

22. Rice, E.J.; and Zaman, K.B.M.Q.: Control of Shear Flows By Artificial Excitation. AIAA Paper 87-2722, Oct. 1987 (Also, NASA TM-100201).

23. Zaman, K.B.M.Q.; McKinzie, Jr., D.J.; and Rumsey, C.L.: A Natural Low-Frequency Oscillation of the Flow Over an Airfoil Near Stalling Conditions. J. Fluid Mech., vol. 202, May 1989, pp. 403-442.

17

24. Durbin, P.A.; and McKinzie, Jr., D.J.: Corona Anemometry For Qualitative Measurement of Reversing Surface Flow with Application to Separation Control by External Excitation. Forum on Unsteady Flow Separation, K.N. Ghia, ed., ASME, 1987, pp. 15-18.

25. Durbin, P.A.; McKinzie, Jr., D.J.; and Durbin, E.J.: An Anemometer for Highly Turbulent or Recirculating Flows. Exper. Fluids, vol. 5, no. 3, 1987, pp. 184-188.

26. Simpson, R.L.; Chew, Y.T.; and Shivaprasad, B.G.: Measurements of a Separating Turbulent Boundary Layer. Project SQUID Rep. SMU-4-PU, Princeton Univ., 1980. (Avail. NTIS, AD-A095252.)

27. Chien, J.C.: Numerical Analysis of Turbulent Separated Subsonic Diffuser Flow. Symposium on Turbulent Shear Flows, vol. 1, Pennsylvania State University, 1977, pp. 18.19-18.25.

28. Ramiz, M.A.; and Acharya, M.: Signatures of Unsteady Separation. AIAA Paper 89-1017, Mar. 1989.

29. Nelson, C.F.; Koga, D.J.; and Eaton, J.K.: Unsteady, Separated Flow Behind an Oscillating Two-Dimensional Spoiler. AIAA J., vol. 28, no. 5, May 1990, pp. 845-852.

30. Miau, J.J.; Chen, M.H.; and Chou, J.H.: Frequency Effect of an Oscillating Plate Immersed in a Turbulent Boundary Layer. AIAA Paper 89-1016, Mar. 1989.

31. Ho, C.M.; and Huang, L.S.: Subharmonic and Vortex Merging in Mixing Layers. J. Fluid Mech., vol. 119, June 1982, pp. 443-473.

32. Oster, D.; and Wygnanski, I.: The Forced Mixing Layer Between Parallel Streams. J. Fluid Mech., vol. 123, Oct. 1982, pp. 91-130.

33. Walker, J.D.A.: The Boundary Layer due to Rectangular Vortex. Proc. R. Soc. London A., vol. 359, no. 1697, Feb. 15, 1978, pp. 167-188.

34. Doligalski, T.L.; and Walker, J.D.A.: The Boundary Layer Induced by a Convected Two-Dimensional Vortex. J. Fluid Mech., vol. 139, Feb. 1984, pp. 1-28.

35. Ersoy, S.; and Walker, J.D.A.: Flow Induced at a Wall by a Vortex Pair. AIAA J., vol. 24, no. 10, Oct. 1986, pp. 1597-1605.

36. Coles, D.: The Law of the Wake in the Turbulent Boundary Layer. J. Fluid Mech., vol. 1, pt. 2, July 1956, pp. 191-226.

37. Deutsch, S.; and Zierke, W.C.: The Measurement of Boundary Layers on a Compressor Blade in Cascade at High Positive Incidence Angle, II - Data Report. NASA CR-179492, 1986.
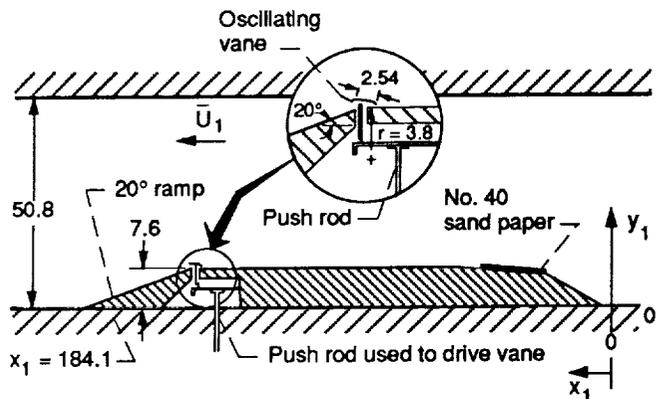
Figure 1.—Side view of 20 degree ramp model in 20 by 30 inch wind tunnel. All dimensions are in centimeters.
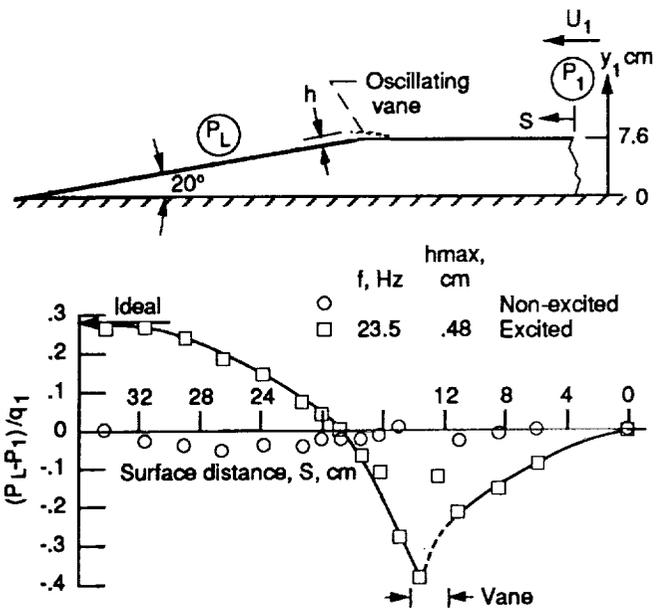
Figure 3.—Static pressure coefficient distribution on ramp for excited and non-excited conditions, U_1 = 2.6m/sec case.
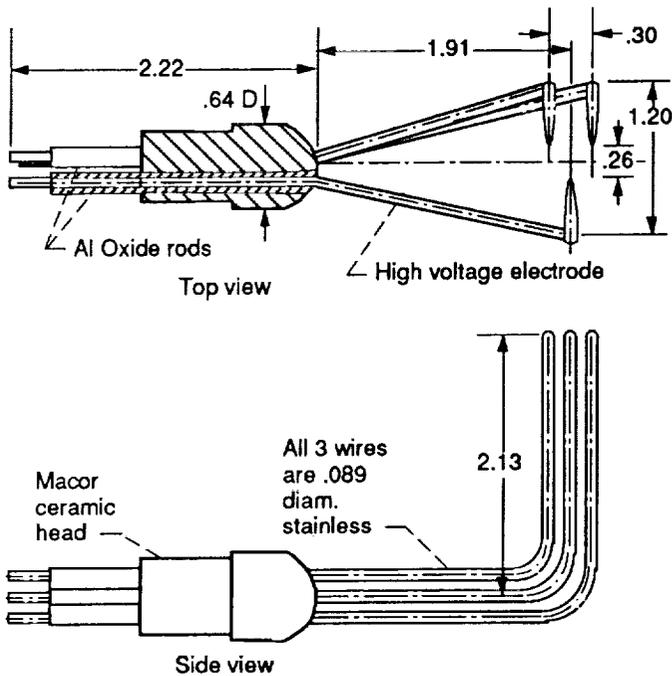

Figure 2.—Working head of corona anemometer. All dimension: in centimeters.
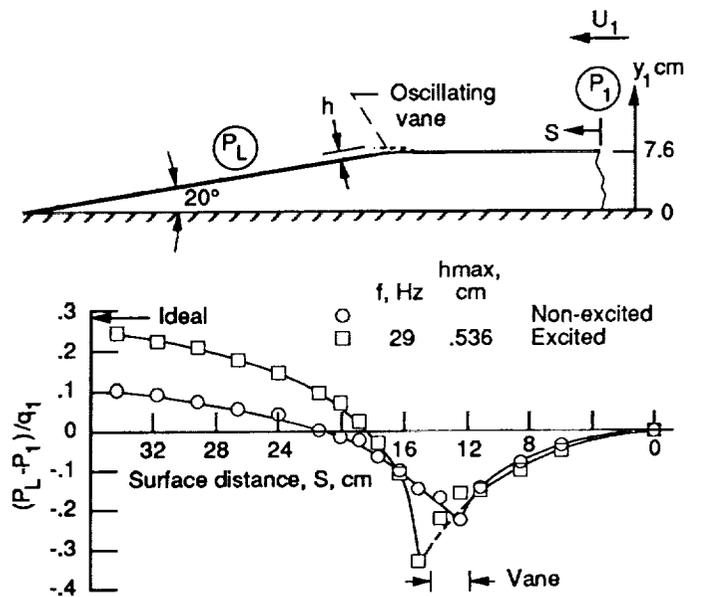
Figure 4.—Static pressure coefficient distribution on ramp for excited and non-excited conditions, $\bar{U}_1$ = 6.6m/sec case.

19
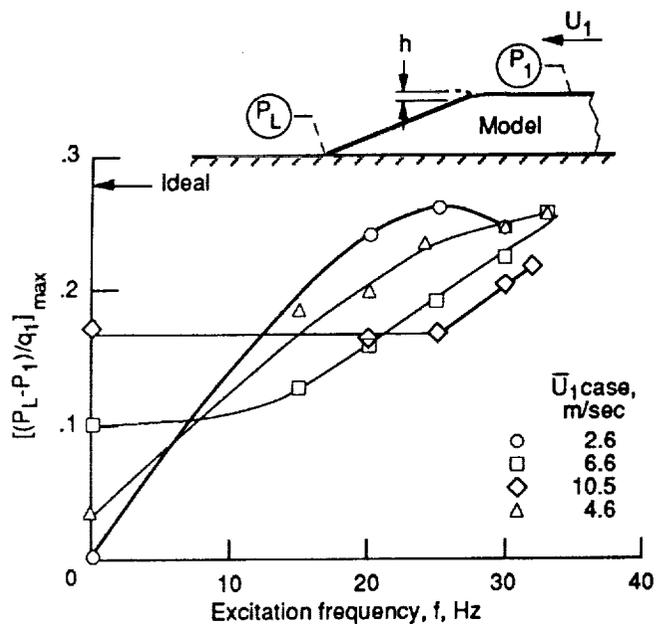
(a) Maximum static pressure recovery as a function of excitation frequency, f, at constant vane displacement height, h, of .318 cm.
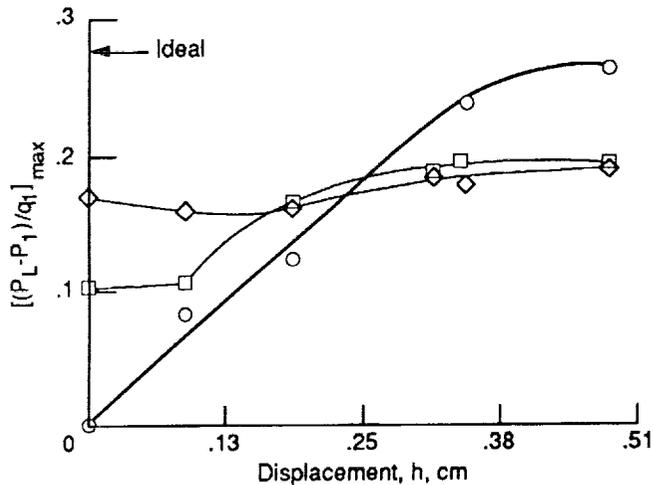
(b) Maximum static pressure recovery as a function of vane displacement height at constant excitation frequency of 24 Hz.

Figure 5.—Maximum static pressure recovery for $\bar{U}_1$ of 2.6, 6.6, 4.6, and 10.5 m/sec.
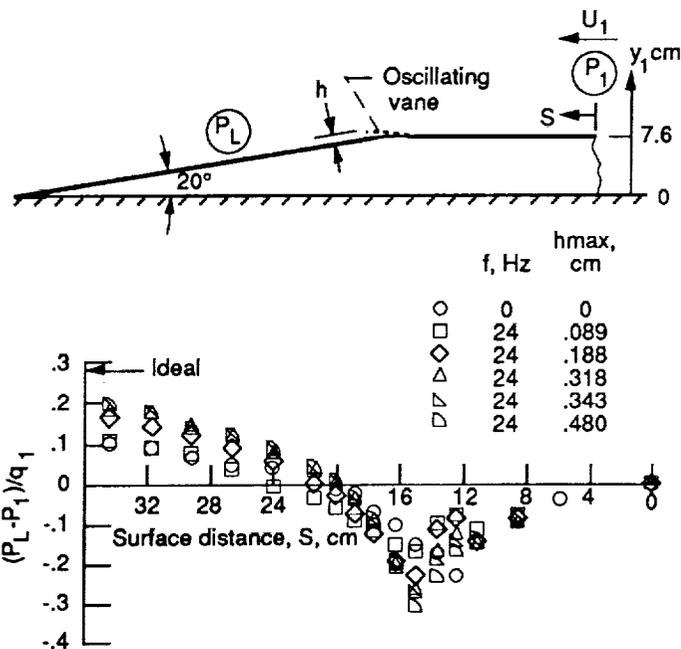
(a) Static pressure recovery on ramp as a function of vane displacement height, h, for constant excitation frequency, f, of 24 Hz.
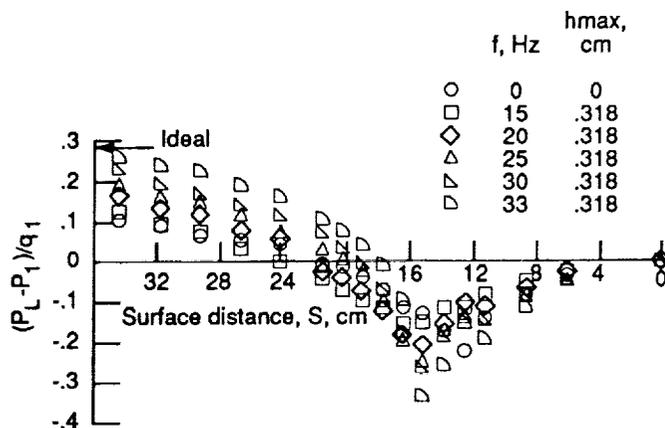
(b) Static pressure recovery on ramp as a function of excitation frequency for constant displacement height of .318 cm.

Figure 6.—Static pressure recovery on ramp for $\bar{U}_1$ of 6.6m/sec.
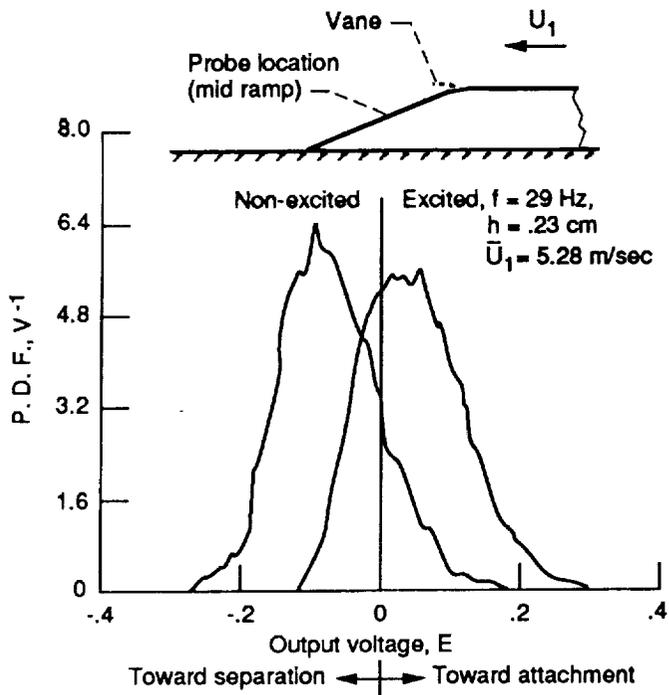
Figure 7.—Typical corona anemometer unsteady velocity probability density distribution as a function of output signal in volts.
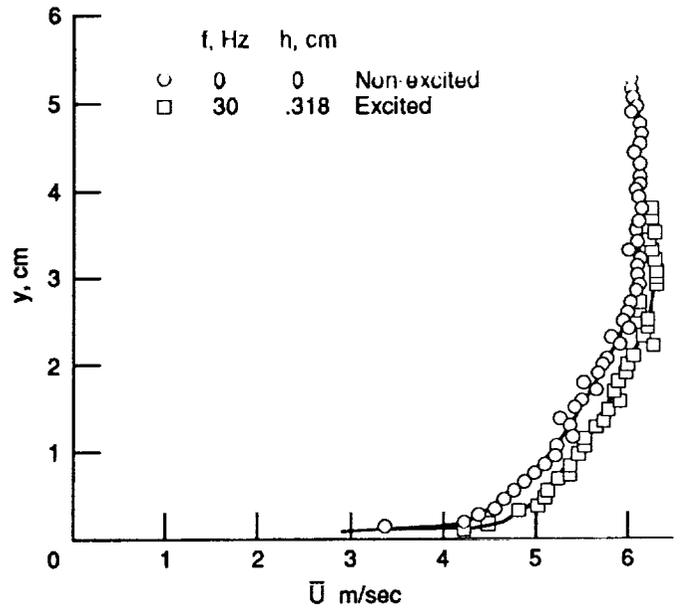
Figure 9.—Comparison of velocity profiles 0.127 cm upstream of vane's hinge point for case of $\bar{U}_1$ = 6.3 m/sec.
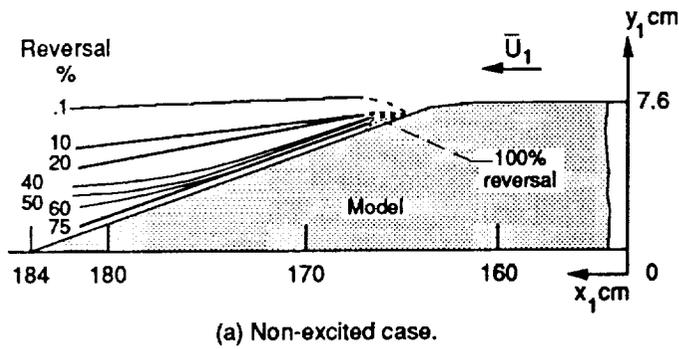
(a) Non-excited case.
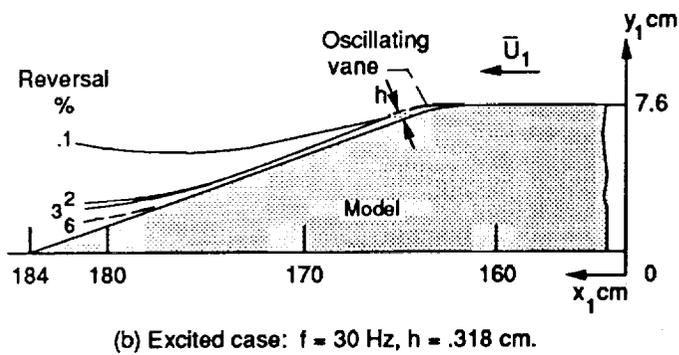
(b) Excited case: f = 30 Hz, h = .318 cm.

Figure 8.—Contours of the averaged flow reversal rate for the non-excited and excited cases for $\bar{U}_1$ = 6.6m/sec.
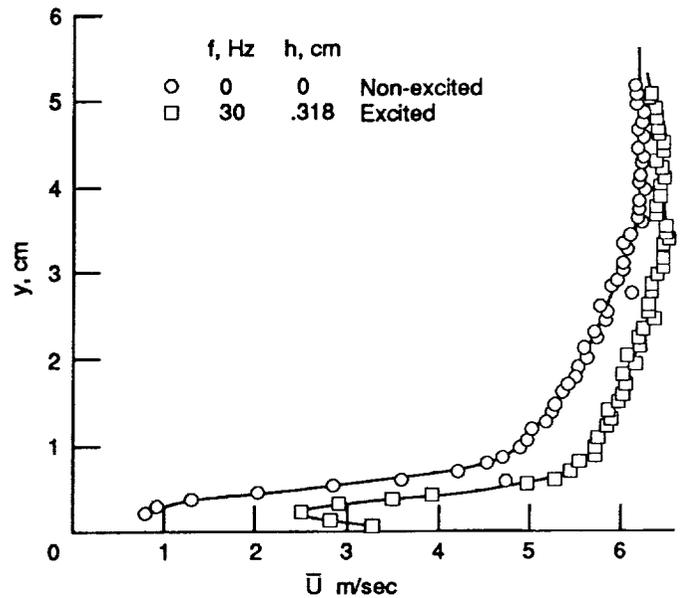
Figure 10.—Comparison of velocity profiles 0.572 cm downstream of vane trailing edge for case of $\bar{U}_1$ = 6.6 m/sec.

21
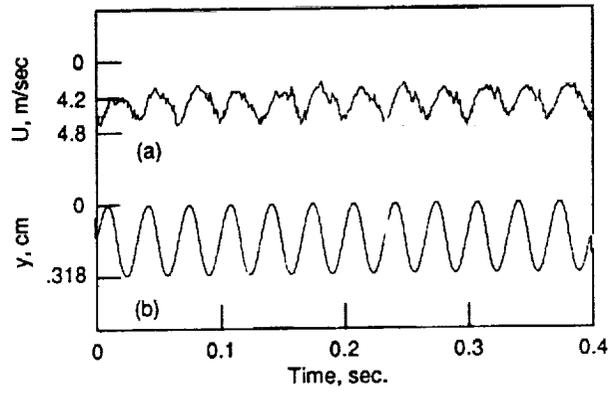
Figure 11.—Wave forms of (a) corona anemometer
real time signal at .476 cm downstream of the
vane's trailing edge and at a height of .152 cm;
(b) accelerometer displacement real time signal,
located on the vane driver mechanism.
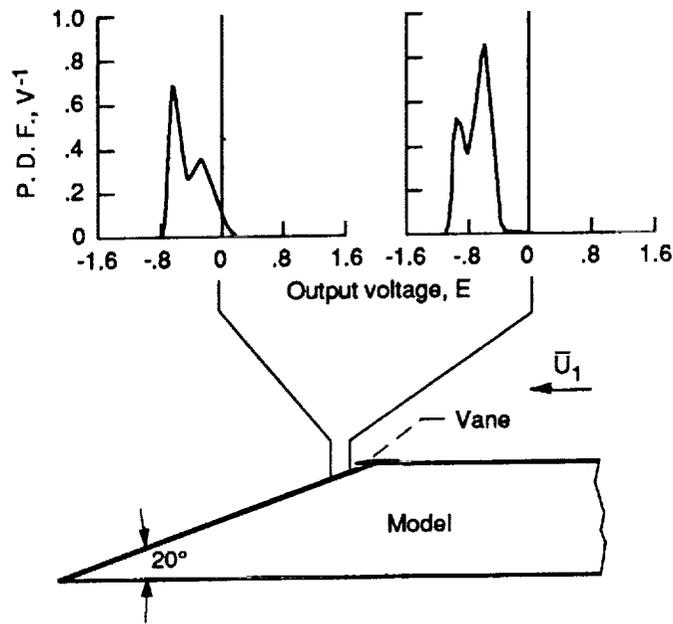
Figure 12.—Corona anemometer probability density versus
output signal at .152 cm. above ramp surface for excited
case, $\bar{U}_1$ of 6.6 m/sec.

22

(a) Non-excited condition, smoke-wire located upstream of
inlet to ramp. Oscillating vane not on model.

(b) Excited condition, smoke-wire located nominally 2.5 cm
downstream of vane's trailing edge. Vane oscillation
frequency, f, is 29 Hz.

Figure 13.—Smoke visualization of flow passing from right
to left over 20 degrees rearward facing ramp. $\bar{U}_1$ = 2.6
m/sec case.
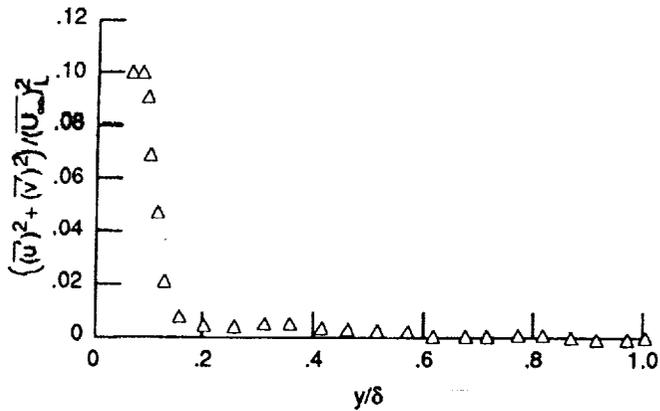
Figure 14.—Turbulent kinetic energy versus y/δ for f = 30 Hz and h = .318 cm at .572 cm downstream of vane trailing edge.
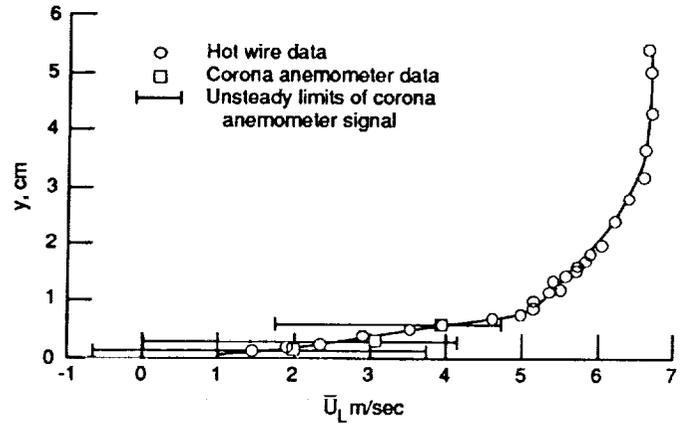
Figure 17.—Velocity profile 1.746 cm downstream of vane trailing edge for $\bar{U}_1$ = 6.6 m/sec case, exited at f = 30 Hz, h = .318 cm.
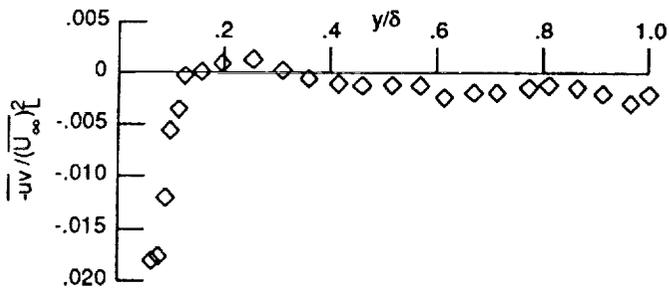
Figure 15.—Reynolds shearing stress $-\bar{uv}/(\bar{U}_\infty)^2_L$ versus y/δ for f = 30 Hz and h = .318 cm at .572 cm downstream of vane trailing edge.
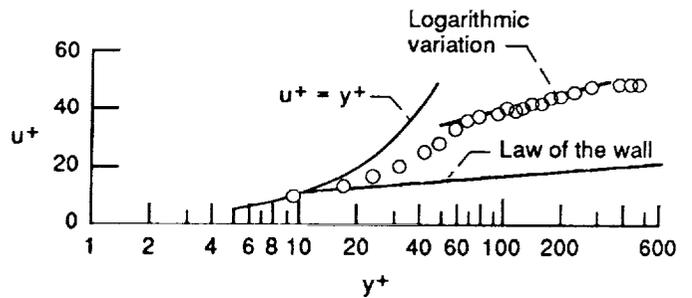

Figure 18.—Velocity profile in inner wall coordinates 1.746 cm downstream of vane trailing edge for $\bar{U}_1$ = 6.6 m/sec case, excited at f = 30 Hz, h = .318 cm.
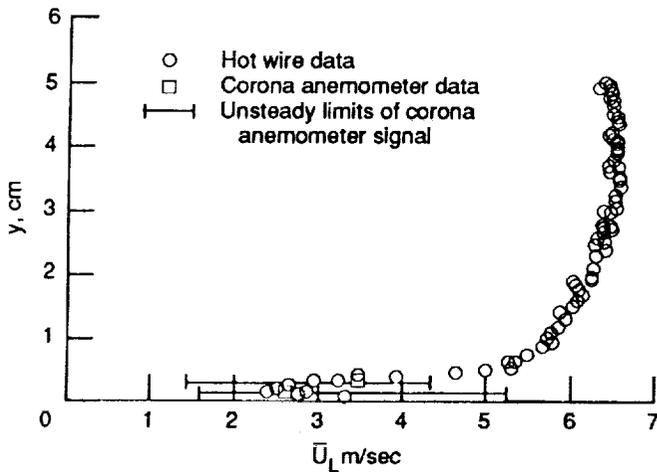

Figure 16.—Velocity profile 0.476 cm downstream of vane trailing edge for $\bar{U}_1$ = 6.6 m/sec case, exited at f = 30 Hz, h = .318 cm.
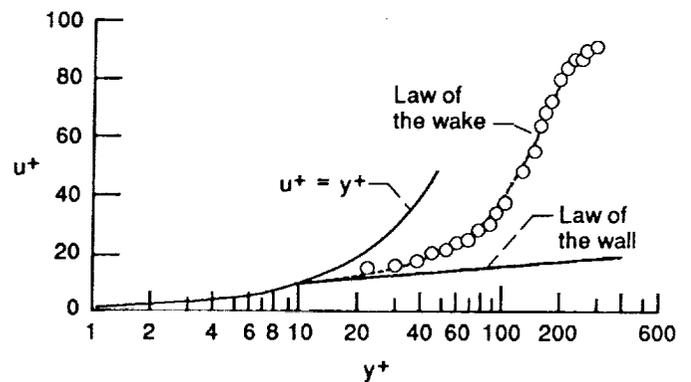

Figure 19.—Velocity profile in inner coordinates 17.1 cm downstream of vane trailing edge for $\bar{U}_1$ = 6.6 m/sec case, excited at f = 30 Hz, h = .318 cm.

24
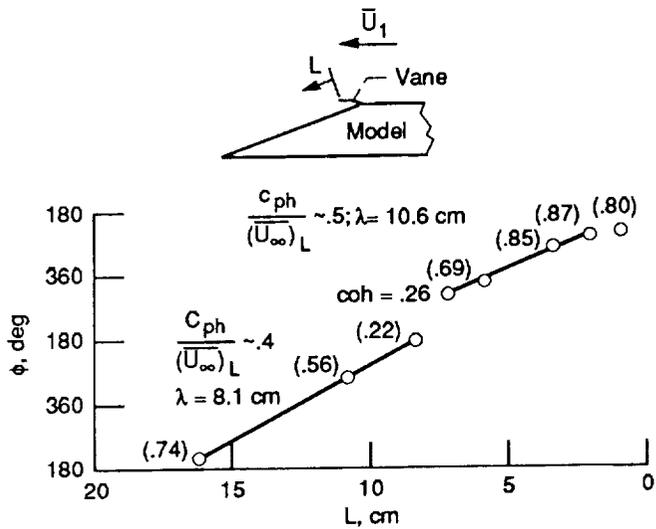
Figure 20.—Phase angle, ϕ, versus L measured from vanes trailing edge. Measurements at 40% $(\overline{U}_\infty)_L$ for $f = 30$ Hz, $h = .318$ cm, and $\overline{U}_1 = 6.6$ m/sec. Coherence is shown in brackets, λ and $C_{ph}/(\overline{U}_\infty)_L$ represent nominal wave length and phase speed, respectively.

(a) .48 cm from vane trailing edge.

(b) 4.44 cm from vane trailing edge.

(c) 8.26 cm from vane trailing edge.
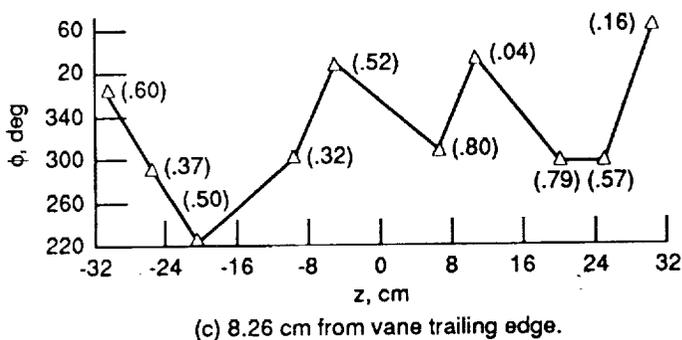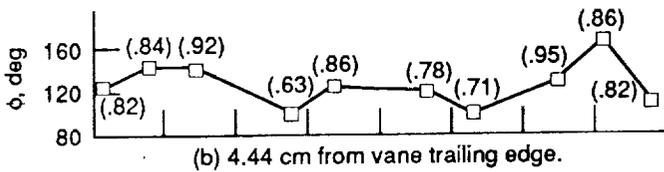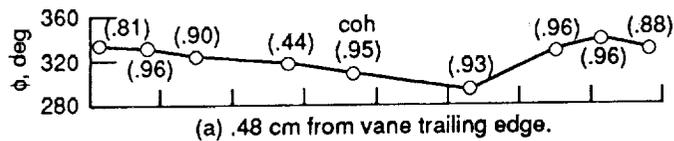
Figure 21.—Variation of phase angle, ϕ, in spanwise direction, z, at axial distance from vane: (a) 0.48 cm, (b) 4.44 cm, and (c) 8.26 cm. Measurements are made at $\overline{U}_L/(\overline{U}_\infty)_L$ of 40%. $\overline{U}_1 = 6.6$ m/sec, $f = 30$ Hz, and $h = .318$ cm. Coherence is shown in brackets.
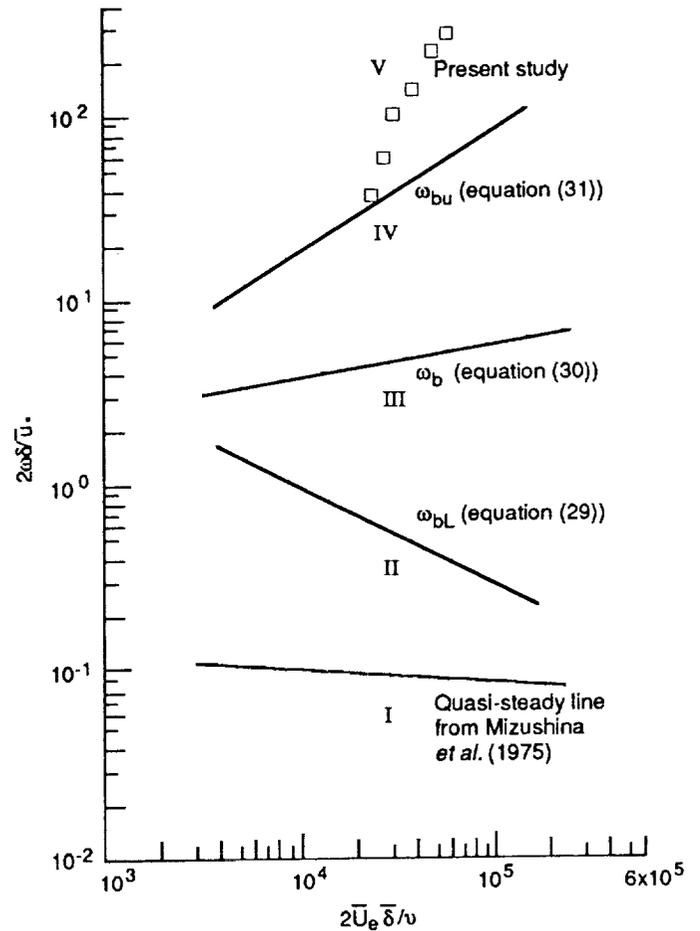
Figure 22.—Classification of unsteady turbulent shear flows from reference 15. Note that, in the case of boundary-layer data, time-mean freestream velocity $\overline{U}_e$ and time-mean boundary-layer thickness $\overline{\delta}$ are used as reference velocity and lengthscales in place of $\overline{U}_m$ and 1/2D, respectively.
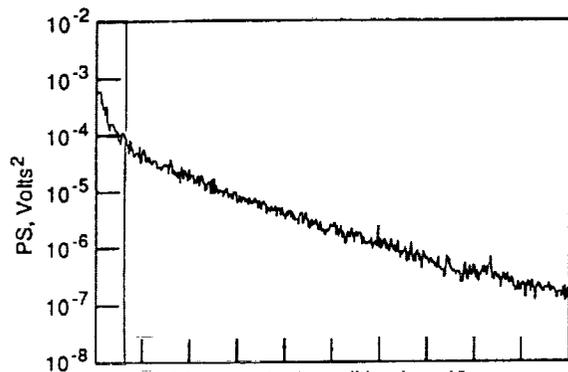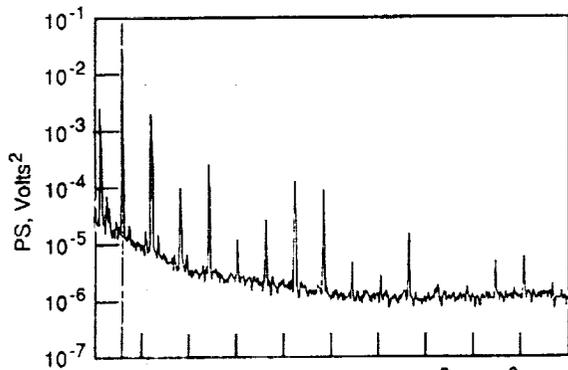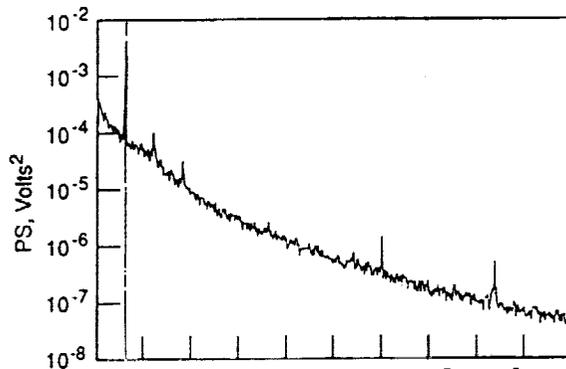
25
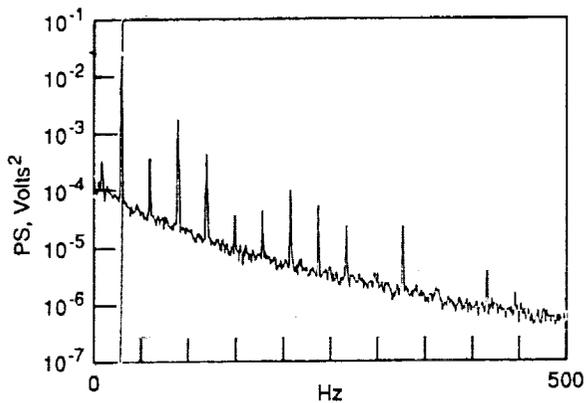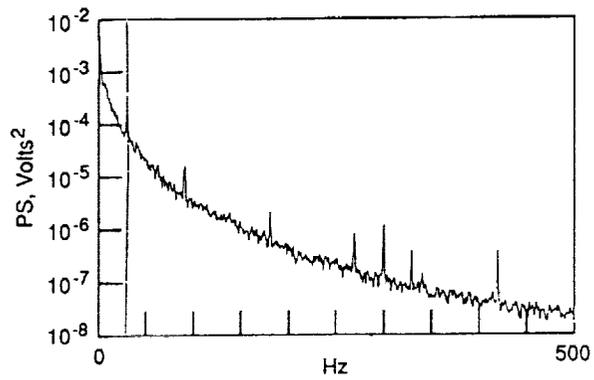
Figure 23.—Power spectra, PS, in volts^2 measured at specific locations, L, from the vane's trailing edge and at .152 cm above the ramp's surface for the 6.6 m/sec case. Cursor values at 30 Hz. (a) Nonexcited condition; vane down on surface. (b-e) Excited condition: f = 30 Hz, h = .318 cm.

Report Documentation Page

1. Report No. NASA TM-103702 AIAA-91-0253	2. Government Accession No.	3. Recipient's Catalog No.
4. Title and Subtitle Turbulent Boundary Layer Separation Over a Rearward Facing Ramp and Its Control Through Mechanical Excitation		5. Report Date
		6. Performing Organization Code
7. Author(s) Daniel J. McKinzie, Jr.		8. Performing Organization Report No. E-5860
		10. Work Unit No. 505-62-21
9. Performing Organization Name and Address National Aeronautics and Space Administration Lewis Research Center Cleveland, Ohio 44135-3191		11. Contract or Grant No.
		13. Type of Report and Period Covered Technical Memorandum
12. Sponsoring Agency Name and Address National Aeronautics and Space Administration Washington, D.C. 20546-0001		14. Sponsoring Agency Code

15. Supplementary Notes

16. Abstract

A vane oscillating about a fixed point at the inlet to a two-dimensional 20 degree rearward facing ramp has proven effective in delaying the separation of a turbulent boundary layer. Measurements of the ramp surface static pressure coefficient obtained under the condition of vane oscillation and constant inlet velocity revealed that two different effects occured with surface distance along the ramp. In the vicinity of the oscillating vane the pressure coefficient varied as a negative function of the vane's trailing edge rms velocity; the independent variables on which the rms velocity depends are the vane's oscillation frequency and its displacement amplitude. From a point downstream of the vane to the exit of the ramp, however, the pressure coefficient varied as a more complex function of the two independent variables. That is, it was found to vary as a function of the vane's oscillation frequency throughout the entire range of frequencies covered during the test, but over only a limited range of the trailing edge displacement amplitudes covered. More specifically, the value of the pressure coefficient was independent of increases in the vane's displacement amplitude above approximately 35 inner wall units of the boundary layer. Below this specific amplitude it varied as a function of the vane's trailing edge rms velocity. This height is close to the upper limit of the buffer layer, indicating that the action of the vane is primarily affecting the buffer and viscous sublayers of the boundary layer. A parametric study was made to determine the variation of the maximum static pressure recovery as a function of the vane's oscillation frequency, for several ramp inlet velocities and a constant displacement amplitude of the vane's trailing edge. The results indicate that the phenomenon producing the optimum delay of separation may be Strouhal number dependent. Corona anemometer measurements obtained in the inner wall regions of the boundary layer for the excited case reveal a large range of unsteadiness in the local velocities. These measurements imply the existence of inflections in the profiles, which provide a mechanism for resulting inviscid flow instabilities to produce turbulence in the near wall region, thereby delaying separation of the boundary layer.

17. Key Words (Suggested by Author(s)) Rearward facing ramp Separation	18. Distribution Statement Unclassified – Unlimited Subject Category 34

19. Security Classif. (of this report) Unclassified	20. Security Classif. (of this page) Unclassified	21. No. of pages 28	22. Price* A03